Experimental Modal Analysis of Angle Signals Based on the Stochastic Subspace Identification Method

IN-HO KIM[1]

[1] Department of Civil Engineering, Kunsan National University, Kunsan 54150, Korea
E-mail: inho.kim@kunsan.ac.kr

Received: November 18 2021, Accepted: January 26, 2022 Published: January 31, 2022

Abstract

This paper aims to verify the results of extraction of modal parameters from angle signals based on stochastic subspace identification (SSI). Angle signal-based mode shape can reduce the loss of node information and increase the robustness of curvature-based damage detection. First, system identification of the angle signal is performed prior to damage detection. In general, excitation of large structures is difficult, so an output-only system identification method is required for modal analysis of angular signals. To achieve this, the SSI method is used. Because it does not deal with non-linear problems, it is one of the most powerful tools for output-only system identification methods. To describe the process of system identification of an angular signal using the SSI method, it is assumed that the transformation matrix represents the relationship between the angular displacement and the normal displacement. Next, a modified block Hankel matrix composed of an angle signal that can be expressed as a product of a transformation matrix and a displacement sequence vector is constructed. The observability matrix can be estimated using singular value decomposition for the projection of the future part onto the past part of the modified block Hankel matrix. Finally, we use the state and observation matrices to compute the eigen-frequency and angular signal-based mode shapes. To verify the analytical study results, the modal characteristics estimated through numerical analysis and the SSI method using angular velocity measurement were compared.

Keywords: system identification, stochastic subspace identification, Hankel matrix, modal analysis, damage detection

Introduction

Most large structures, such as bridges, nuclear power plants, buildings, and offshore platforms, may be exposed to unexpected loads during their lifetime. In particular, serious events such as earthquakes, overloaded traffic jams, and typhoons can cause deterioration of structures. In order to prevent catastrophic damage to large structures, vibration-based damage detection research is receiving a lot of attention [1-3]. Vibration-based damage assessment can be performed by examining changes in the modal properties of a structure, such as natural frequency and modal shape. Therefore, system identification for estimating dynamic modal characteristics is a very important part in vibration-based damage detection.

However, artificial vibration excitation or shock excitation is virtually impossible for large structures. Structures can be vibrated by ambient input sources such as traffic, wind, etc. In other words, system identification for large structures that use input and output sources is not very practical because the surrounding input sources are unknown. To solve this problem, many researchers have proposed output-only system identification methods.

Felber [4] implemented a peak selection method using all output signals and a reference sensor node. In this approach, the natural frequency can be simply estimated as the peak of the spectrum obtained by transforming the time domain signal into a frequency domain signal using a discrete Fourier transform technique. The autoregressive moving average vector (ARMAV) model has also been used to identify output-only systems [5]. The autoregressive (AR) portion of the output is coupled with the moving average (MA) portion of the white noise input. Based on the output signal, the prediction error approach [6] can estimate an unknown system matrix.

However, this approach has drawbacks in terms of inaccuracy and non-linear problems. The stochastic subspace identification (SSI) method has been considered as one of the most powerful tools for identification of output-only systems because it does not deal with nonlinear problems. Therefore, the SSI approach is much faster, more accurate and more robust than the previous method. For this reason, the SSI method has been studied further in the past decades [7-10]. In particular, the book published by van Overschee and De Moor [11] marked a breakthrough in SSI. Finally, the modal parameters estimated from the SSI method can be used for vibration-based damage detection.

Recently, curvature-based damage detection approaches [12-15] have received considerable attention as one of the most sensitive and reliable vibration-based approaches. However, the existing curvature-based approach has limitations in damage localization because it requires double differentiation and curve fitting of the displacement mode shape to calculate the mode shape curvature. On the other hand, if the angle signal-based mode shape used is extracted from the angle signal, the curvature can be calculated simply by using one derivative (displacement mode shape □ angle signal based mode shape □ mode shape curvature). Through this process, the loss of node information can be reduced and the robustness according to the curvature estimation can be improved. In this regard, in order to obtain an angle signal-based mode form, system identification using an angle signal should be performed first.

In this study, the method of estimating the angle signal-based mode shape using the SSI method using the angle signal was investigated. The purpose of this study is to verify the performance of the proposed method by comparing the angular signal-based mode shape and angular velocity obtained by the SSI method through computer simulations and experiments. Chapter 2 compares the block Hankel matrix for generalized acceleration, velocity, and displacement with the block Hankel matrix for generalized angular acceleration, angular velocity, and angular displacement. Next, modal analysis is performed from the estimated system matrix using the future block Hankel matrix and the past block Hankel matrix. Chapter 3 compares the results of the numerical analysis and the experimental modal analysis. Chapter 4 concludes this task.

https://doi.org/10.24949/njes.v14i2.672

Theory

2.1. Block Hankel matrix for generalized acceleration, velocity, and displacement

A continuous-time state-space model of a dynamic system with respect to acceleration, velocity, and displacement can be expressed as

$$\dot{\mathbf{z}}_y(t) = \mathbf{A}_{cy}\mathbf{z}_y(t) + \mathbf{B}_{cy}\mathbf{f}(t), \quad (1)$$

$$\mathbf{y}(t) = \mathbf{C}_{cy}\mathbf{z}_y(t), \quad (2)$$

where $\mathbf{z}_y = \begin{Bmatrix} x \\ \dot{x} \end{Bmatrix}$, x is the displacement, and $\dot{x}$ is the velocity. The state matrix ($\mathbf{A}_{cy}$) and the load matrix ($\mathbf{B}_{cy}$) are given by:

$$\mathbf{A}_{cy} = \begin{bmatrix} \mathbf{0} & \mathbf{I} \\ -\mathbf{M}^{-1}\mathbf{K} & -\mathbf{M}^{-1}\mathbf{C} \end{bmatrix}, \quad \mathbf{B}_{cy} = \begin{bmatrix} \mathbf{0} \\ \mathbf{M}^{-1} \end{bmatrix} \quad (3)$$

where M, K and C are the structural mass, stiffness and damping matrices, respectively.

From the previous study [8], the discrete solution of $\mathbf{y}(k)$ can be obtained simply as follows:

$$\mathbf{y}(k) = \mathbf{C}_y \mathbf{A}_y^k \mathbf{z}(0). \quad (4)$$

The stochastic subspace identification begins by constructing the block Hankel matrix ($\mathbf{H}_y$) as follows:

$$\mathbf{H}_y = \begin{bmatrix} \mathbf{y}_1 & \mathbf{y}_2 & \cdots & \mathbf{y}_{N-2s} \\ \mathbf{y}_2 & \mathbf{y}_3 & \cdots & \mathbf{y}_{N-2s+1} \\ \vdots & \vdots & \ddots & \vdots \\ \mathbf{y}_{2s} & \mathbf{y}_{2s+1} & \cdots & \mathbf{y}_N \end{bmatrix} = \begin{bmatrix} \mathbf{H}_{yp} \\ \mathbf{H}_{yf} \end{bmatrix}, \quad (5)$$

where the subscript "p" indicates the "past" and the subscript "f" indicates the "future". Thus, $\mathbf{H}_{yp}$ and $\mathbf{H}_{yf}$ are the block Hankel matrices including the past outputs and future outputs, respectively.

Block Hankel matrix for generalized angular acceleration, angular velocity, and angular displacement

Similar to equations (1) and (2), the continuous time state space model related to angular acceleration, angular velocity, and angular displacement can be expressed as follows:

$$\dot{\mathbf{z}}_\theta(t) = \mathbf{A}_{c\theta}\mathbf{z}_\theta(t) + \mathbf{B}_{c\theta}\mathbf{f}(t), \quad (6)$$

$$\boldsymbol{\theta}(t) = \mathbf{C}_{c\theta}\mathbf{z}_\theta(t), \quad (7)$$

where $\mathbf{z}_\theta = \begin{Bmatrix} \theta \\ \dot{\theta} \end{Bmatrix}$, θ is the angular displacement, and $\dot{\theta}$ is the angular velocity.

Assume that a linear transformation between the angular displacement (θ) and the displacement (y) exists as follows [16]:

$$\boldsymbol{\theta} = \mathbf{T}\mathbf{y}, \quad (8)$$

where $\mathbf{T}$ is the transformation matrix.

Thus, the block Hankel matrix ($\mathbf{H}_\theta$) for generalized angular acceleration, angular velocity, and angular displacement can be expressed as follows:

$$\mathbf{H}_\theta = \begin{bmatrix} \boldsymbol{\theta}_1 & \boldsymbol{\theta}_2 & \cdots & \boldsymbol{\theta}_{N-2s} \\ \boldsymbol{\theta}_2 & \boldsymbol{\theta}_3 & \cdots & \boldsymbol{\theta}_{N-2s+1} \\ \vdots & \vdots & \ddots & \vdots \\ \boldsymbol{\theta}_{2s} & \boldsymbol{\theta}_{2s+1} & \cdots & \boldsymbol{\theta}_N \end{bmatrix} = \begin{bmatrix} \mathbf{Ty}_1 & \mathbf{Ty}_2 & \cdots & \mathbf{Ty}_{N-2s} \\ \mathbf{Ty}_2 & \mathbf{Ty}_3 & \cdots & \mathbf{Ty}_{N-2s+1} \\ \vdots & \vdots & \ddots & \vdots \\ \mathbf{Ty}_{2s} & \mathbf{Ty}_{2s+1} & \cdots & \mathbf{Ty}_N \end{bmatrix} = [\backslash \mathbf{T} \backslash]\mathbf{H}_y. \quad (9)$$

Finally, the upper half and lower half of the block Hankel matrix ($\mathbf{H}_\theta$) can be obtained as follows:

$$\begin{bmatrix} \mathbf{H}_{\theta p} \\ \mathbf{H}_{\theta f} \end{bmatrix} = [\backslash \mathbf{T} \backslash] \begin{bmatrix} \mathbf{H}_{yp} \\ \mathbf{H}_{yf} \end{bmatrix}, \quad (10)$$

where $\mathbf{H}_{\theta p}$ and $\mathbf{H}_{\theta f}$ are the upper half and lower half of the block Hankel matrix including the past outputs and future outputs, respectively.

Projection

Van Overchee and De Moor [11] introduced a projection technique as a geometrical tool. However, for stochastic responses, projection is defined as a conditional mean ($\mathbf{O}_y$), as follows [8]:

$$\mathbf{O}_y = \mathrm{E}(\mathbf{H}_{yp} \mid \mathbf{H}_{yp}) = \mathbf{H}_{yf}\mathbf{H}_{yp}^{\mathrm{T}}(\mathbf{H}_{yp}\mathbf{H}_{yp}^{\mathrm{T}})^{-1}\mathbf{H}_{yp} \quad (11)$$

From equation (4), the matrix $\mathbf{O}_y$ can be expressed as follows [8]:

$$\mathbf{O}_y = \mathbf{P}_y \mathbf{z}(0), \quad (12)$$

where $\mathbf{P}_y$ is the observability matrix, which is given by:

$$\mathbf{P}_y = \begin{bmatrix} \mathbf{C}_y \\ \mathbf{C}_y\mathbf{A}_y \\ \mathbf{C}_y\mathbf{A}_y^2 \\ \vdots \\ \mathbf{C}_y\mathbf{A}_y^{s-1} \end{bmatrix}. \quad (13)$$

The projection ($\mathbf{O}_\theta$) of the future block Hankel matrix ($\mathbf{H}_{\theta f}$) onto the past block Hankel matrix ($\mathbf{H}_{\theta f}$) can be defined as follows:

$$\mathbf{O}_\theta = \mathrm{E}(\mathbf{H}_{\theta p} \mid \mathbf{H}_{\theta p}) = [\backslash \mathbf{T} \backslash]\mathbf{H}_{yf}\mathbf{H}_{yp}^{\mathrm{T}}[\backslash \mathbf{T} \backslash]^{\mathrm{T}}([\backslash \mathbf{T} \backslash]\mathbf{H}_{yp}\mathbf{H}_{yp}^{\mathrm{T}}[\backslash \mathbf{T} \backslash]^{\mathrm{T}})^{-1}[\backslash \mathbf{T} \backslash]\mathbf{H}_{yp} = [\backslash \mathbf{T} \backslash]\mathbf{O}_y. \quad (14)$$

Using equations (12), (13), and (14), the projection ($\mathbf{O}_\theta$) can be reconstructed as follows:

$$\mathbf{O}_\theta = [\backslash \mathbf{T} \backslash]\mathbf{P}_y\mathbf{z}(0) = \begin{bmatrix} \mathbf{TC}_y \\ \mathbf{TC}_y\mathbf{A}_y \\ \mathbf{TC}_y\mathbf{A}_y^2 \\ \vdots \\ \mathbf{TC}_y\mathbf{A}_y^{s-1} \end{bmatrix} \mathbf{z}(0) = \mathbf{P}_\theta \mathbf{z}(0). \quad (15)$$

The state matrix can be calculated from the estimate of the reconstructed observability matrix ($\mathbf{P}_\theta$) by removing the first block and the bottom block, which yields the following:

$$\begin{bmatrix} \mathbf{TC}_y \\ \mathbf{TC}_y\mathbf{A}_y \\ \mathbf{TC}_y\mathbf{A}_y^2 \\ \vdots \\ \mathbf{TC}_y\mathbf{A}_y^{s-2} \end{bmatrix} \mathbf{A} = \begin{bmatrix} \mathbf{TC}_y\mathbf{A}_y \\ \mathbf{TC}_y\mathbf{A}_y^2 \\ \mathbf{TC}_y\mathbf{A}_y^3 \\ \vdots \\ \mathbf{TC}_y\mathbf{A}_y^{s-1} \end{bmatrix}. \quad (16)$$

The important aspect to consider is the estimated state matrix (**A**). Although system identification is performed using the observability matrix ($\mathbf{P}_\theta$), the estimated state matrix is the matrix $\mathbf{A}_y$, not the matrix $\mathbf{A}_\theta$, as described in equation (16). In contrast, the observation matrix C can be obtained as follows:

$$\mathbf{C} = \mathbf{P}_\theta(1:1) = \mathbf{T}\mathbf{C}_y. \quad (17)$$

Modal analysis

Finally, the modal parameters can be extracted from the estimated system matrix matrix ($\mathbf{A}_y$) and the observation matrix (**C**). In order to achieve the eigenvalue, an analysis of the state matrix $\mathbf{A}_y$ is performed as follows:

$$\mathbf{A}_y = \mathbf{\Psi}_y[\mu_i]\mathbf{\Psi}_y^{-1}, \quad (18)$$

$$f_i = \frac{\left|\ln(\mu_i)/\Delta\mathrm{T}\right|}{2\pi}, \quad (19)$$

$$\mathbf{\Phi} = \mathbf{C}\mathbf{\Psi}_y = \mathbf{TC}_y\mathbf{\Psi}_y = \mathbf{T}\mathbf{\Phi}_y = \mathbf{\Phi}_\theta, \quad (20)$$

where f_i is the i-th natural frequency, $\mathbf{\Phi}_y$ is the displacement mode shape, and $\mathbf{\Phi}_\theta$ is the angle signal-based mode shape.

From the modal analysis, the structural natural frequencies were estimated using state matrix $\mathbf{A}_y$, as described in equation (18). Thus, the estimated natural frequencies are identical to the values that are obtained from the accelerations, velocities, and displacements. However, the angle signal-based mode shapes were obtained (not displacement mode shapes), as depicted in equation (20).

COMPARATIVE STUDY

To verify the analytical study results, the modal analysis results of the SSI method were compared using the modal parameters estimated from the numerical analysis and the dynamic response obtained through the experiment. Numerical simulations were performed using MATLAB. In the experiment, a MEMS-type gyroscope was used to measure the angular velocity because the gyroscope is inexpensive and has good performance. Specifications of the same numerical and experimental models are given in Table 1. The sensor location and structural dimensions are shown in Figure 1.

Table 1. Structural model properties.

Properties	Value
Damping ratio	0.01
Mass density (kg m-3)	7850
Poisson's ratio	0.28
Elasticity modulus (Gpa)	200
Length (m)	2.04
Width (mm)	100
Thickness (mm)	10

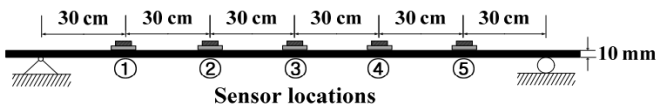

Figure 1. Sensor locations for comparative study

Numerical simulation

From equation (8), the relationship between the displacement mode shape ($\mathbf{\Psi}_y$) and angle signal-based mode shape ($\mathbf{\Psi}_\theta$) is expressed as follows:

$$\mathbf{\Psi}_\theta = \mathbf{T}\mathbf{\Psi}_y. \quad (21)$$

The transformation matrix (**T**) for the numerical simulation is calculated using static condensation. Consider a system following the Euler-Bernoulli beam theory. Assume that the system can be simulated as a lumped-mass matrix. Then, its element stiffness matrix can be expressed as follows:

$$[\mathbf{K}^e] = \frac{EI}{L^3}\begin{bmatrix} 12 & 6L & -12 & 6L \\ 6L & 4L^2 & -6L & 2L^2 \\ -12 & -6L & 12 & -6L \\ 6L & 2L^2 & -6L & 4L^2 \end{bmatrix}\begin{Bmatrix} y_1 \\ \theta_1 \\ y_2 \\ \theta_2 \end{Bmatrix}. \quad (22)$$

Then, the equation of motion can be expressed in partitioned-matrix form as follows [17]:

$$\begin{bmatrix} \mathbf{M}_{yy} & \mathbf{0}_{y\theta} \\ \mathbf{0}_{\theta y} & \mathbf{0}_{\theta\theta} \end{bmatrix}\begin{Bmatrix} \ddot{\mathbf{U}}_y \\ \ddot{\mathbf{U}}_\theta \end{Bmatrix} + \begin{bmatrix} \mathbf{K}_{yy} & \mathbf{K}_{y\theta} \\ \mathbf{K}_{\theta y} & \mathbf{K}_{\theta\theta} \end{bmatrix}\begin{Bmatrix} \mathbf{U}_y \\ \mathbf{U}_\theta \end{Bmatrix} = \begin{Bmatrix} \mathbf{P}_y(t) \\ \mathbf{0} \end{Bmatrix}, \quad (23)$$

where $\mathbf{U}_y$ is the displacement vector and $\mathbf{U}_\theta$ is the rotational displacement vector. From the lower partition of equation (23), $\mathbf{U}_y$ can be transformed into $\mathbf{U}_\theta$ follows:

$$\mathbf{U}_\theta = \left[-\mathbf{K}_{\theta\theta}^{-1}\mathbf{K}_{\theta y}\right]\mathbf{U}_y = \mathbf{T}\mathbf{U}_y. \quad (24)$$

Thus, the displacement mode shape $\mathbf{\Psi}_y$ can be transformed to a angle signal-based mode shape $\mathbf{\Psi}_\theta$ using the transformation matrix $\left[-\mathbf{K}_{\theta\theta}^{-1}\mathbf{K}_{\theta y}\right]$. The estimated angle signal-based mode shapes from the numerical simulation are compared with the angle signal-based mode shapes obtained from experiment in Section 3.2.

Experiment

To obtain modal characteristics such as natural frequency and angular signal-based mode shape, angular velocity was measured using five analog gyroscopes (model: LPY503AL, STMicroelectronics) installed in a simple beam model as shown in Figure 1. For comparative studies, two different types of excitation tests were performed: ambient excitation and shock excitation. Vibration measurements were performed for 150 s at a sampling frequency of 150 Hz. The time domain and frequency domain signals of angular velocity for each excitation test are shown in Figures 2 and 3. Table 2 presents the estimated natural frequencies from the three tests. A comparative study was conducted to verify the results of the analytical study (Chapter 2) by comparing the angular signal-based mode shape obtained through numerical analysis with the experiment. By normalizing the maximum value of each

angle signal-based mode shape to one, the first two angle signal-based mode shapes were compared as shown in Figure .

4. The SSI method using the angular velocity obtained through computer simulation and experiment was almost the same

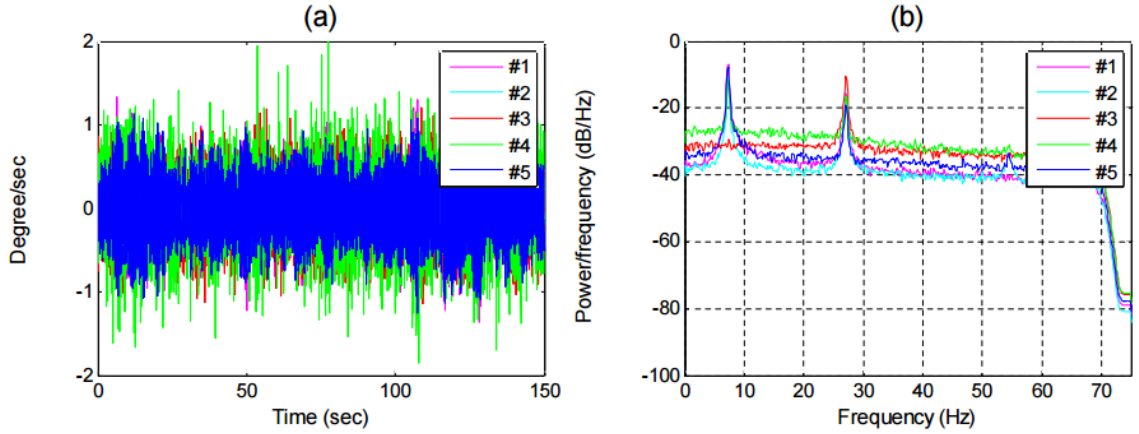

Figure 2. Angular-velocity responses: (a) time domain (b) frequency domain (for ambient excitation)

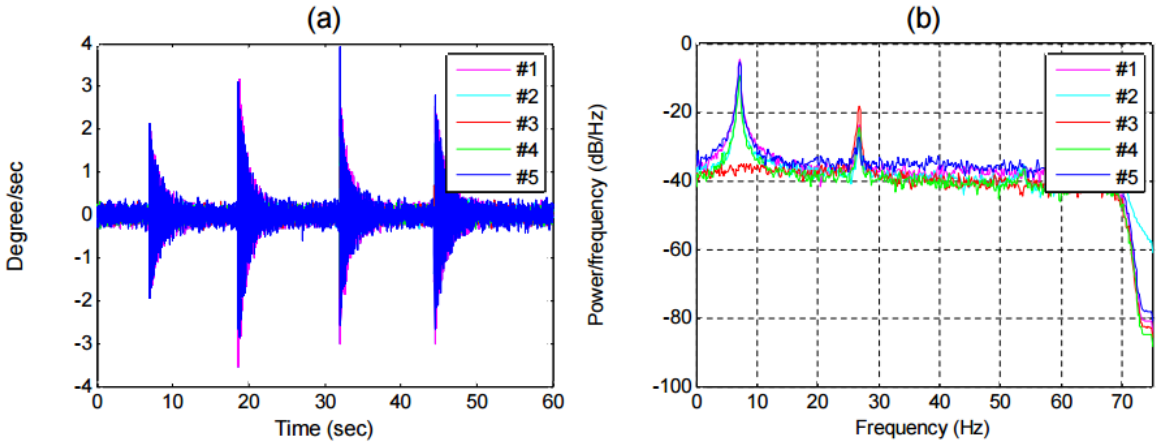

Figure 3. Angular-velocity responses: (a) time domain (b) frequency domain (for impact excitation)

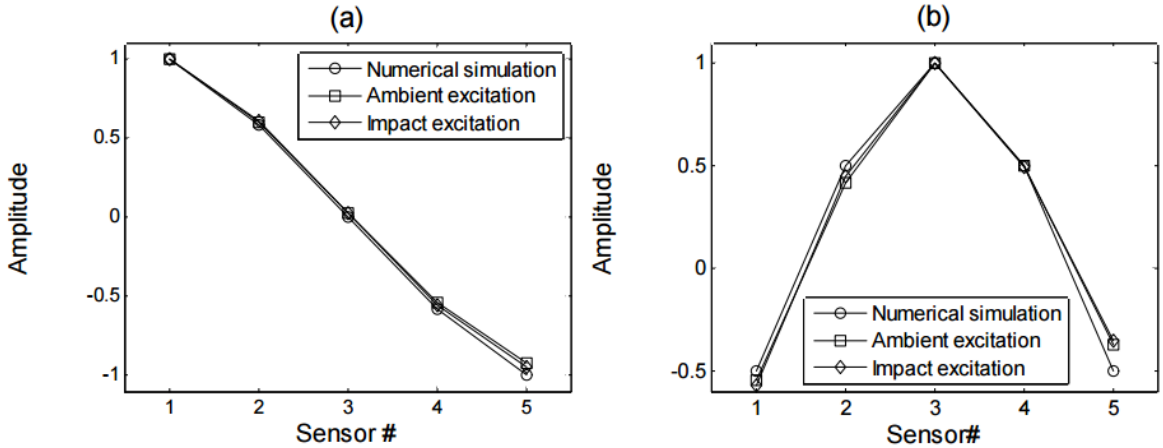

Figure 4. Angle signal-based mode shapes (a) the first mode (b) the second mode (for each case)

Table 2. Estimated natural frequencies.

	Case		
	Numerical simulation	Ambient excitation	Impact excitation
First mode: f1 (Hz)	7.05 (100%)	7.27 (103.1%)	7.24 (102.7%)
Second mode: f2 (Hz)	28.04 (100%)	27.14 (96.8%)	26.86 (95.8%)

Conclusions

In this paper, we analytically investigated the process of obtaining modal parameters from angle signals using the SSI method. Existing curvature-based damage detection approaches using displacement-mode features have limitations in damage localization because they require the double derivative of the displacement-mode features to calculate the modal feature curvature. However, the use of angle-signal-based modal shapes can compensate for the weakness of curvature-based approaches using displacement-mode shapes due to simple differentiation (displacement-mode shape angle-signal-based mode shape mode shape curvature). To achieve this, system identification of the angle signal must be performed prior to damage detection. In this study, since it is virtually impossible to excite a large structure using a shaker or impact load, the SSI method was used as an output-only system identification method for modal analysis of angle signals. The transformation matrix was assumed to express the relationship between the angular displacement and the normal displacement. Next, a modified block Hankel matrix composed of an angle signal that can be expressed as a product between a transformation matrix and a displacement sequence vector was constructed. We then performed a projection of the future part onto the past part of the modified block Hankel matrix. The observability matrix was estimated through the singular value decomposition on the projection. Finally, the mode shape based on the natural frequency and angle signal was estimated using the state matrix and the observation matrix composed of the observability matrix. To verify the analytical study results, the modal characteristics estimated by the SSI method using numerical analysis and angular velocity measurement were compared. As a result of comparison, it was found that the shape of the angular signal-based mode obtained by the SSI method using the angular velocity obtained through computer simulation and experiment is almost the same.

Acknowledgments

This research was supported by Basic Science Research Program through the National Research Foundation (NRF) funded by the Ministry of Education (No. NRF-2020R1I1A1A01073676)

References

1. S.W. Doebling, C.R. Farrar, M.B. Prime, D.W. Shevitz, “Damage identification and health monitoring of structural and mechanical systems from changes in their vibration characteristics: a literature review”, Los Alamos National Lab. (LANL), Los Alamos, NM, Tech. Rep. LA-13070-MS, May. 1996.
2. H. Sohn, C.R. Farrar, F.M. Hemez, D.D. Shunk, D.W. Stinemates, B.R. Nadler, “A Review of structural health monitoring literature: 1996–2001”, Los Alamos National Lab. (LANL), Los Alamos, NM, Tech. Rep. LA-UR-02-2095, Jan. 2002.
3. W. Fan, P. Qiao, “Vibration-based damage identification methods: a review and comparative study”, *Structural Health Monitoring*, Vol. 10, 2011, pp. 83-111.
4. A. J. Felber, “Development of a hybrid bridge evaluation system”, Ph.D. thesis, University of British Columbia, Vancouver, Canada, 1993.
5. J. B. Bodeux and J. C. Golinval, “Application of ARMAV models to the identification and damage detection of mechanical and civil engineering structures”, *Smart Materials and Structures*, Vol. 10, 2001, pp. 1-10.
6. L. Ljung, “System identification: Theory for the user”, Prentice Hall, USA, 1987.
7. B. Peeters, G. De Roeck, “Reference-based stochastic subspace identification for output-only modal analysis”, *Mechanical Systems and Signal Processing*, Vol. 13, 1999, pp. 855-878.
8. R. Brincker, P. Andersen, “Understanding stochastic subspace identification”, *Proceedings of the 24th IMAC: A Conference & Exposition on Structural Dynamics.*, Society for Experimental Mechanics, St. Louis, Missouri, 2006.
9. E. Reynders, R. Pintelon, G. De Roeck, “Uncertainty bounds on modal parameters obtained from stochastic subspace identification”, *Mechanical Systems and Signal Processing*, Vol. 22, 2008, pp. 948-969.
10. B. Moaveni, E. Asgarieh, “Deterministic-stochastic subspace identification method for identification of nonlinear structures as time-varying linear systems”, *Mechanical Systems and Signal Processing*, Vol. 31, 2012, pp. 40-55.
11. P. van Overschee, B. De Moor. “Subspace identification for linear systems”, Kluwer Academic Publishers, Netherlands, 1996
12. M. M. AbdelWahab, G. DeRoeck, “Damage detection in bridges using modal curvatures: application to a real damage scenario”, *Journal of Sound and Vibration*, Vol. 226, 1999, pp. 217-235.
13. W. Lestari, P. Qiao, S. Hanagud, “Curvature mode shape-based damage assessment of carbon/epoxy composite beams”, *Journal of Intelligent Material Systems and Structures*, Vol. 18, 2007, pp. 189-208.
14. M. Cao, M. Radzienski, W. Xu, W. Ostachowicz, “Identification of multiple damage in beams based on robust curvature mode shapes”, *Mechanical Systems and Signal Processing*, Vol. 46, 2014, pp. 468-480.
15. S. H. Sung, K. Y. Koo, H. J. Jung, “Damage detection for beam-like structures using the normalized curvature of a uniform load surface”, *Journal of Sound and Vibration*, Vol. 332, 2013, pp. 1501-1519.
16. S. H. Sim, B. F. Spencer, Jr, T. Nagayama, “Multimetric sensing for structural damage detection”, *Journal of Engineering Mechanics*, Vol. 137, 2011, pp. 22-30.
17. R. R. Craig, A. J. Kurdila, “Fundamentals of structural dynamics” 2nd edition. Wiley, USA, 2006.